

STELLAR TOOLS FOR HIGH RESOLUTION POPULATION SYNTHESIS

M. Chávez,¹ E. Bertone,¹ L. H. Rodríguez-Merino,¹ and A. Buzzoni²

RESUMEN

Presentamos los resultados preliminares de la aplicación de una nueva biblioteca estelar de espectros sintéticos de alta resolución (con base en los códigos ATLAS9 y SYNTHE desarrollados por Kurucz) para el cálculo de la distribución de energía espectral en el ultravioleta-óptico de poblaciones estelares simples (SSPs). Para este propósito, la biblioteca se acopló con el código de síntesis de poblaciones de Buzzoni. Una parte de este artículo está dedicada a ilustrar de manera cuantitativa el grado al cual las bibliotecas estelares sintéticas representan a las estrellas reales.

ABSTRACT

We present preliminary results of the application of a new stellar library of high-resolution synthetic spectra (based upon ATLAS9 and SYNTHE codes developed by R. L. Kurucz) in the calculation of the ultraviolet-optical spectral energy distribution of simple stellar populations (SSPs). For this purpose, the library has been coupled with Buzzoni's population synthesis code. Part of this paper is also devoted to illustrate quantitatively the extent to which synthetic stellar libraries represent real stars.

Key Words: STARS: ATMOSPHERES — ULTRAVIOLET: STARS

1. INTRODUCTION

Evolutionary population synthesis is undoubtedly the most popular method to analyze the integrated spectrophotometric properties of stellar systems. Most works dealing with Mid-UV and optical wave ranges have implemented Kurucz theoretical stellar fluxes (Kurucz 1995) to cope with the deficiency of empirical libraries in covering the parameter space at sub-solar metallicity regimes. However the low resolution (10 Å in the UV and 20 Å in the optical) makes this grid not suitable to fully exploit the high-quality observations provided by new instruments, such as the spectrographs onboard FUSE, HST or those attached to the 8m-class telescopes. For instance, it has been claimed that some of the limitations of Kurucz library of model fluxes might well be part of the reasons of the discrepant results when dating elliptical galaxies at high redshift (Nolan et al. 2003). We are currently developing a project aimed at constructing a large data base at increased resolution for population synthesis studies. In this contribution we present, in Sec. 5, some preliminary results of applying our high resolution stellar library within Buzzoni's synthesis code (Buzzoni 1989) and illustrate the behavior of features in two spectral bands, one in the Mid-UV and the wavelength interval defining the Mg2 index.

In this paper we also show the results of the quantitative comparison between synthetic stellar spectra and observed data. Such a comparison has been quite often neglected in the literature, however, it is of fundamental importance for validating (or invalidating) the use of theoretical spectral in a variety of astronomical branches (Bell, Paltoglou & Tripicco, 1994; Bertone et al. 2004a).

2. THE STELLAR GRID

The full wavelength interval (850–7000 Å) for our models is covered by two distinct grids of synthetic spectra (one centered on the ultraviolet range, and the other tuned in the optical window). The UV and optical grids were computed separately and mainly differ in the spectral resolution, which is $R=50\,000$ in the UV and $R=500\,000$ in the optical. The main characteristics of the combined grid are given in Table 1 of Bertone et al. (2003). The parameter space covered by the ultraviolet grid UVBLUE is depicted in Figure 1 where we plot the grid points (for solar metallicity) in the $\log g - \log T_{\text{eff}}$ diagram, together with open symbols indicating the position of stars in the catalogue of Wu et al. (1983) and a set of evolutionary tracks (Girardi et al. 2000; Salasnich et al. 2000) for stars ranging from 0.6 to 15 M_{\odot} . A similar plot for the optical grid can be found in Bertone et al. (2004b).

Both grids used as input the Kurucz ATLAS9 model atmospheres (Kurucz 1995). The high-resolution spectra were computed using the SYN-

¹INAOE, Tonantzintla, México.

²INAF-Osservatorio Astronomico di Bologna, Italy.

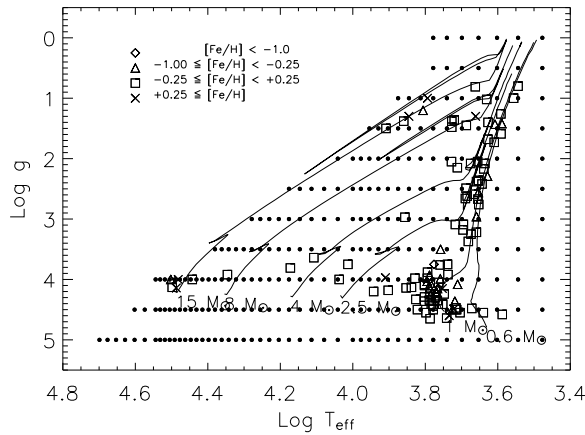


Fig. 1. Parameter space covered by UVBLUE. Open symbols stand for stars included in the Wu et al. (1983) atlas. Note the homogeneous coverage of the synthetic grid.

THE series of codes by Kurucz (1993). Line opacity derives from the huge database of Kurucz (1992) which includes all atomic elements at different ionization states and several diatomic molecules (namely, C2, CN, CO, CH, NH, OH, MgH, SiH, H₂, and SiO). As a major improvement, in our optical spectra we also accounted in some detail for the TiO contribution, relying on the updated work by Schwenke (1998). This new line database provides a more accurate description of the band absorption in the optical range. Quite importantly, the TiO can strongly affect the continuum region around the 5170 MgH feature in M and late-K stars. This has a direct impact when computing Lick spectrophotometric indices, such as Mg2, from theoretical spectra.

In order to account for the effects of stars cooler than 4000 K, we have included a collection of model fluxes extracted from the NextGen spectral library (Hauschildt et al. 1999a, 1999b) down to 2000 K.

3. THEORY VS. OBSERVATIONS: THE ULTRAVIOLET

With the goal of quantitatively compare UVBLUE entries with observational material and establish the extent to which theoretical spectra represent real stars, we have selected IUE spectra of all stars included in the catalogue of Wu et al. (1983) and reprocessed the images (the selection and reprocessing is explained in full detail in Rodríguez-Merino et al. (2004)). We have then identified spectral regions that must not be incorporated into the comparison. The region shortward of 1250 Å has not been included because most of the absorption in the

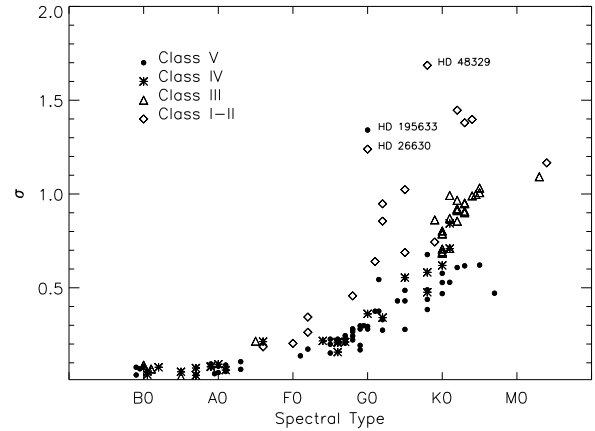


Fig. 2. Summary of the comparison between IUE data and linearly interpolated synthetic spectra within UVBLUE. Different symbols correspond to different luminosity classes. It is evident the gradual increase of the rms toward later spectral types. Discrepancies are enhanced for low gravity objects.

prominent Ly α feature present in observational data of hot stars (most O and B and some A-type) might have interstellar origin (Brandt et al. 1998; Diplas & Savage 1994). We have also excluded spectral regions where IUE data are close to the sensitivity limit (i.e. with very low signal-to-noise ratio). These spectral regions, evidently, will depend on the natural decline of the stellar flux, hence on effective temperature. For intermediate and late-type stars the spectral regions included for the comparison started at 1850 Å for A-type stars, 2100 Å for F, G, K and M stars.

Prior to the comparison we performed some procedures devoted to match the instrumental characteristics of IUE spectra:

- We degraded theoretical spectra to the overall nominal resolution of IUE low-dispersion spectra, 6 Å.
- We resampled theoretical fluxes by linear interpolation in order to match the wavelength points of INES data.
- We linearly interpolated within UVBLUE to produce theoretical spectra for the set of parameters associated to each star. These parameters have been selected from the literature as explained in Rodríguez-Merino et al. (2004).
- The observed fluxes were corrected for extinction using Mathis (1990) law for $R_V = 3.1$ and the set of colour excesses given in Fanelli et al. (1992). (1983).

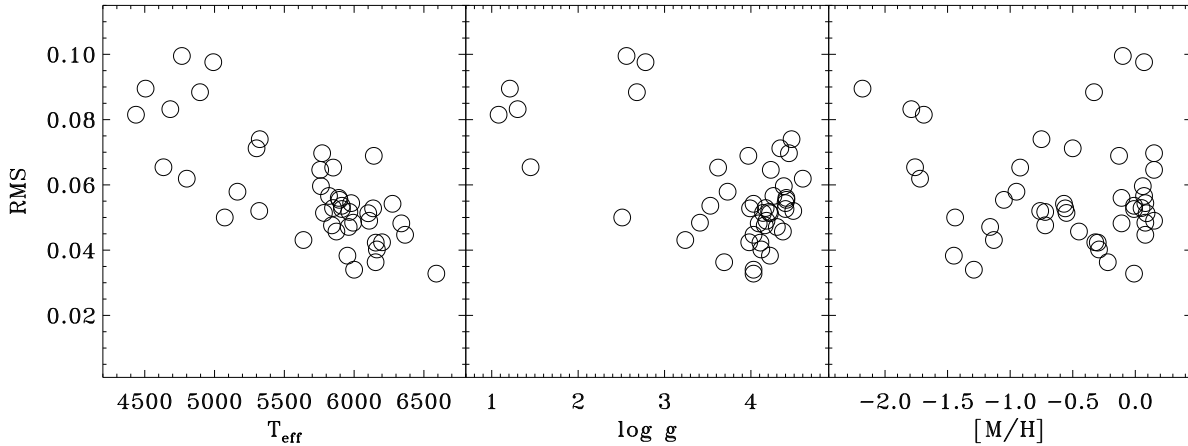


Fig. 3. Comparison between synthetic and observed spectra in the 4100–6800 Å interval. The rms is given as a function of the effective temperature (*left panel*), surface gravity (*central panel*) and metallicity (*right panel*).

- Finally, the observed and theoretical absolute flux levels were made compatible by matching the average fluxes in two 100 Å-wide windows centered in 1700 Å and 2200 Å for SW and LW, respectively, and the theoretical flux were scaled to IUE levels.

The overall result of comparing observed and synthetic fluxes is displayed in Figure 2. The y axis correspond to the rms of the residual logarithmic flux [$\Delta\text{flux} = \ln(\text{synthetic flux}) - \ln(\text{observed flux})$] which gives an estimation of the percentual discrepancies. It is interesting to note the sharp increase in rms toward late spectral types, in particular for low gravities. Although the discrepancies in Figure 2 show that giant and supergiant G, K and M stars are poorly reproduced, they also tell us that UVBLUE can be confidently used for the study of dwarf stars and dwarf-dominated stellar populations, such as early-type galaxies whose UV flux is dominated by stars at the turn-off.

4. THEORY VS OBSERVATIONS: THE VISIBLE

In a similar way as in the previous section, we have performed a detailed comparison with the flux calibrated spectra of the Prugniel & Soubiran (2001) library. The spectra were obtained with the ELODIE echelle spectrograph at the Observatoire de Haute-Provence. They cover the wavelength range 4100–6800 Å at an inverse resolution of $R = 10\,000$. The broadband photometric precision is of the order of 2.5%. These properties make this empirical library suitable to characterize the qualities of our synthetic grid in the optical range.

From the empirical catalogue, we selected the stars having the best flux calibration and the

most reliable physical parameters (the uncertainties should be lower than 80 K in T_{eff} and 0.06 dex in $[M/H]$). We took into account only this subset of stars in order to minimize the contribution of the errors on the physical parameters assigned to each stars to the uncertainty of the comparison with the theoretical SEDs. The final set of 45 F and G-type reference stars covers a T_{eff} interval between 4437 and 6589 K, while the gravity goes from $\log g = 1.08$ to 4.6 dex, and the metallicity ranges from $[Fe/H] = -2.18$ to 0.15.

For each star, a synthetic spectrum with the correspondent combination of T_{eff} , $\log g$, and $[M/H]$ was created by performing a trilinear interpolation within the library. We then broadened the synthetic to the observed spectral resolution. We exclude from the analysis several small intervals (5680–5695, 5859–5985, 6270–6325, 6510–6525, 6735–6755 Å) because of the presence of discontinuities in the observations probably due to the match between echelle orders. The rejection includes, in particular, the NaD doublet.

In Figure 3 is reported the root mean square (rms) of the comparisons as a function of the main physical parameters. The match is becoming increasingly poor towards lower effective temperature and the rms have an average higher value for giant and supergiant stars. Nevertheless, the amount of metals does not seem to influence the quality of the comparison.

5. THE UV-OPTICAL MORPHOLOGY OF SSPS

We have used Buzzoni’s (1989) synthesis code to calculate the integrated spectra for simple stellar populations (SSP) of solar chemical composi-

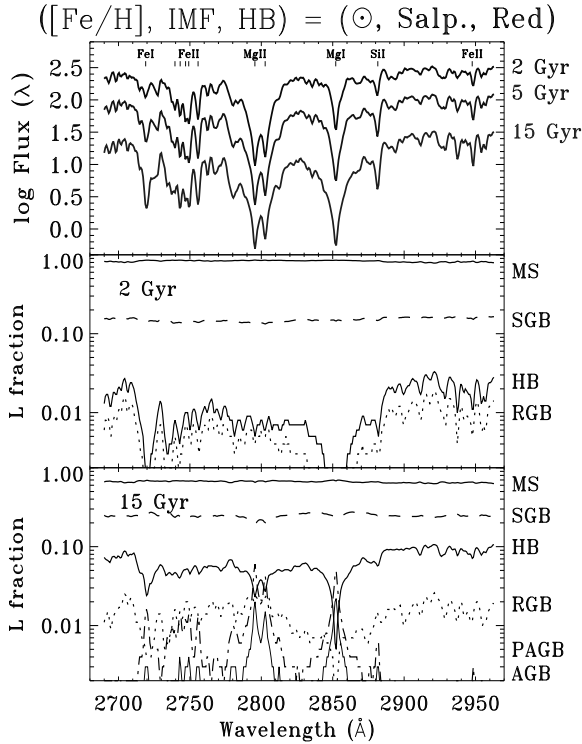


Fig. 4. Integrated Mid-UV spectra for SSPs (*upper panel*) of solar chemical composition. For the calculations we considered a salpeter IMF and a red horizontal branch morphology. For clarity we plot only three ages. In the *middle and lower panels* we plot the contribution to the total luminosity of the different evolutionary stages.

tion. This code includes all important evolutionary phases: main sequence (MS), sub-giant branch (SGB), red giant branch (RGB), horizontal branch (HB), asymptotic giant branch (AGB), and post-asymptotic giant branch (PAGB). For the calculation we have considered nine ages: 2, 3, 4, 5, 6, 8, 10, 12.5 and 15 Gyr, three different slopes of the initial mass function (IMF): $s = 2.35$ (Salpeter), 1.35 and 3.35 and two mass-loss efficiencies given by the Reimers' parameter $\eta = 0.30$ and 0.50. Additionally, Buzzoni's code includes three different HB morphologies: intermediate (I-HB), red (R-HB) and blue (B-HB) (see Buzzoni 1989 for details). The full stellar library has been broadened applying a Gaussian filter of $\text{FWHM} = 2 \text{ \AA}$.

The following figures show some of the results obtained so far. We illustrate the behavior in terms of age of a SSP of several spectral features in two wave bands; one in the Mid-UV (2690–2960 \AA) and one in the optical (4880–5390 \AA). In all cases we have considered a red horizontal branch (R-HB) morphology,

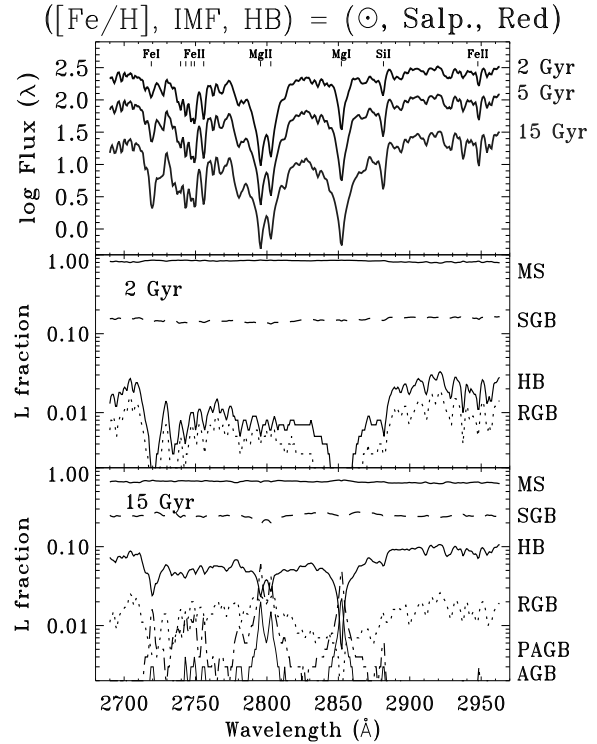


Fig. 5. Same as Fig. 4 for the region around the strong magnesium feature at 5170 \AA .

a Salpeter IMF ($s = 2.35$) and solar chemical composition. In the upper panels of Figures 4 and 5 we plot the evolution of the integrated spectra at three different ages (2, 5 and 15 Gyr). In the two bottom panels (for each band) we present the relative contributions of the different evolutionary phases to the total luminosity of populations at two different ages.

It is interesting to note that while in the optical the dominance of main sequence stars is preserved along the age sequence from 2 to 15 Gyr, in the Mid-UV evolved He-burning stars are dominant in the older population reaching almost 99% at the shorter wavelengths. The HB in the region centered in the Mg feature at 5170 \AA contributes approximately the same as the RGB and the subgiant branch SGB, which is 15% each.

We would like to stress that the material here presented is based on a purely theoretical approach. A detailed comparison of the stellar grid with a homogeneous set of UV-optical data is underway. Similarly we are currently conducting the calculation of SSPs over the entire wavelength interval (850–7000 \AA), other HB morphologies and several metallicities.

This work received partial financial support from the Italian MURST under grant COFIN00 02-016 and from Mexican CONACyT via grant 36547-E.

REFERENCES

- Bell, R. A., Paltoglou, G., & Tripicco, M. J. 1994, *MNRAS*, 268, 771
- Bertone, E., Buzzoni, A., Rodríguez-Merino, L. H., & Chávez, M. 2003, in *IAU Symp. 210, Modelling of Stellar Atmospheres*, ed. N. E. Piskunov, W. W. Weiss & D. F. Gray, (ASP: San Francisco), CDROM A1
- Bertone, E., Buzzoni, A., Chávez, M., & Rodríguez-Merino, L. H. 2004a, *AJ*, in press
- Bertone, E., Buzzoni, A., Rodríguez-Merino, L. H., & Chávez, M. 2004b, in *Stars in Galaxies*, ed. M. Bellazzini, A. Buzzoni, & S. Cassisi, *Mem. SAIT*, 75, 158
- Brandt, J. C., Heap, S. R., Beaver, E. A., et al. 1998, *AJ*, 116, 941
- Buzzoni, A. 1989, *ApJS*, 71, 817
- Diplas, A., & Savage, B. D. 1994, *ApJS*, 93, 211
- Fanelli, M. N., O'Connell, R. W., Burstein & Wu, C. 1992, *ApJS*, 82, 197
- Girardi, L., Bressan, A., Bertelli, G., & Chiosi, C. 2000, *A&AS*, 141, 371
- Hauschildt, P. H., Allard, F., & Baron, E. 1999a, *ApJ*, 512, 377
- Hauschildt, P. H., Allard, F., Ferguson, J., Baron, E., & Alexander, D. R. 1999b, *ApJ*, 525, 871
- Kurucz, R. L. 1992, *RevMexAA*, 23, 45
- Kurucz, R. L. 1993, CD-ROM No. 18, *SYNTHE Spectrum Synthesis Programs and Line Data* (Cambridge: SAO).
- Kurucz, R. L. 1995, CD-ROM No. 13, *ATLAS9 Stellar Atmosphere Programs and 2 km/s Grid* (Cambridge: SAO), revised
- Mathis, J. S. 1990, *ARA&A*, 28, 37
- Nolan, L. A., Dunlop, J. S., Jimenez, R., & Heavens, A. F. 2003, *MNRAS*, 341, 464
- Prugniel, Ph., & Soubiran, C., 2001, *A&A*, 369, 1048
- Rodríguez-Merino, L. H., et al. 2004, in preparation
- Salasnich, B., Girardi, L., Weiss, A., & Chiosi, C. 2000, *A&A*, 361, 1023
- Schwenke, D. W. 1998, *Faraday Discuss.*, 109, 321
- Wu, C.-C., Ake, T. B., Boggess, A., et al. 1983, *The IUE Ultraviolet Spectral Atlas*, Greenbelt: NASA-GSFC.

M. Chávez, E. Bertone, and L. Rodríguez-Merino: Instituto Nacional de Astrofísica, Óptica y Electrónica, Luis Enrique Erro 1 Tonantzintla, Puebla, CP72840, México (mchavez, ebertone, lino@inaoep.mx).

Alberto Buzzoni: INAF-Osservatorio Astronomico di Bologna, Via Ranzani 1, 40127, Bologna, Italy (alberto.buzzoni@bo.astro.it).